

# Methods for space line localization from single catadioptric images: new proposals and comparisons.

Vincenzo Caglioti, Simone Gasparini, Pierluigi Taddei  
Politecnico di Milano  
Dipartimento di Elettronica e Informazione  
Piazza Leonardo da Vinci, 32  
I-20133 Milano (MI), Italy  
{name.surname}@polimi.it

## Abstract

*Line localization from a single image of a central camera is an ill-posed problem unless other constraints or a priori knowledge are exploited. Recently, it has been proved that noncentral catadioptric cameras allow space lines to be localized from a single image.*

*In this paper we propose two novel localization algorithms. The first method exploits a pair of coplanar viewing rays to localize the space line. The second method follows a constrained non-linear minimization procedure using a suitable parametrization to represent space lines.*

*We compare the accuracy of the proposed method w.r.t. the classical line localization algorithm and two robust variants of it. We carried out both synthetic and real experiments and evaluated the performance in localizing a set of space lines. We also propose a quality index for the viewing surfaces associated to space lines in order to better evaluate the quality of the localization.*

*The experimental results showed the effectiveness and the accuracy of both proposed methods.*

## 1. Introduction

Line localization from a single image is an ill-posed problem, as the classical central projection model introduces an ambiguity: the viewing surface, *i.e.* the union set of the viewing rays associated to the line image, is a planar surface that contains infinite line segments (precisely,  $\infty^2$ ) crossing all the viewing rays. The ambiguity can be solved by exploiting additional information in the scene [8], planar [15] or rigidity [17] constraints or by employing stereopsis, which, on the other hand, requires to solve the correspondences problem.

In order to reconstruct a line from single images, we have to employ optical systems whose image formation is not a

central projection. Catadioptric cameras are optical devices constituted by a standard perspective camera placed in front of a curved, axial symmetric mirror. Since the viewing rays are reflected by the mirror, the image formation model is altered so that, in general, it is no more a central projection. Baker and Nayar [2] have derived the complete class of central catadioptric cameras which preserves the single viewpoint constraint, preventing line localization as well. Central catadioptric cameras can be obtained by placing the camera viewpoint in one of the foci of a mirror based on a quadric of revolution. However these cameras are not easy to manufacture since require a precise alignment of the camera that is also difficult to check.

Noncentral catadioptric cameras, on the other hand, are a more general class of cameras whose viewing rays are not all concurrent: thus they can be exploited as multi-viewpoint systems to reconstruct lines from single images.

As observed by Caglioti and Gasparini [6] the only viewing surfaces that hinder line localization are planar viewing surfaces (PVS), since they contain infinite ( $\infty^2$ ) lines other than the viewing rays, and Ruled Quadrics viewing surfaces (RQVS), since they contain infinite ( $\infty^1$ ) lines other than the viewing rays. If a viewing surface is neither a PVS nor a RQVS, then the line can be localized with at most two distinct solutions [9]. Under broad conditions, a significant set of space lines can be localized in the 3D space for both axial symmetric and off-axis cameras as shown in [6].

If a space line can be localized, the reconstruction algorithm reduces to the determination of the transversal to the set of viewing rays associated to the image line. Bronnmann *et al.* [4] shows that given a set of viewing rays (not lying on a PVS or QRVS) there are at most two transversals crossing all the rays. Moreover, according to a classical geometric property by Hilbert [9], four viewing rays are sufficient to determine the two transversals. Teller and Hohmeyer [16] were the first to propose a method based on

Plücker representation to determine the transversals to four lines for computer graphics application. Lately, the technique was resumed by Avidan *et al.* [1] to reconstruct the 3D coordinates of a moving point seen from a monocular moving camera, and by Lanman *et al.* [10] to reconstruct a line from a single image taken by a catadioptric camera based on a spherical mirror.

The localization accuracy of these methods suffers from the small baselines between rays. Moreover, in classical adopted mirror shapes, the viewing surfaces of space lines tend to be close to ruled quadrics. In order to tackle these issues, more robust methods are needed or, at least, catadioptric systems exploiting multiple projection of the same line are required, as in [10].

We investigate the former approach. In particular the original contributions of this work are: (i) two novel line localization algorithms, one exploiting a pair of coplanar viewing rays, and the other one using a constrained non-linear optimization procedure based on a suitable Plücker representation of the space lines; (ii) a comparison of the effectiveness and the robustness of the proposed methods w.r.t. classical algorithms; (iii) a quality index for the viewing surfaces associated to space lines in order to better evaluate the quality of the localization.

The paper is organized as it follows. In Section 2 we address the problem and formulate our assumptions. In Section 3 we briefly recall the classical localization method showing two robust variants, one based on a minimization procedure and the other on RANSAC algorithm. Then we propose two novel approaches, one exploiting a pair of coplanar viewing rays (Section 4), and one using a non-linear minimization procedure (Section 5). In Section 7 we present and discuss the experimental results obtained with the different methods.

## 2. Problem formulation

We consider a calibrated noncentral catadioptric camera based on a convex mirror placed in a general position w.r.t. the camera, so that some space lines (satisfying the conditions stated in [6]) are visible through the mirror. Given a catadioptric image captured with such a system, we suppose that the curve  $c$  representing the image of a space line have been extracted. Notice that, for the purpose of this paper, we are not interested in how the lines is detected on the image. Then, since the whole system is calibrated, we determine all the viewing rays associated to each point of  $c$ .

## 3. Localization from four viewing rays

The classical localization algorithm proposed in [16] employs only four viewing rays. From classical geometry, given a set of  $N > 3$  skew viewing rays, they either form a ruled quadric (a hyperboloid of one sheet or a hyperbolic

paraboloid), and thus have infinite ( $\infty^1$ ) transversals, or they have at most two transversals [9]. In the latter case, the two transversals can be determined by using four rays. Since the space lines we consider does not lie neither on a QRVS nor on a PVS, we can chose any four viewing rays in order to localize the line up to two solutions. The feasible one can be then disambiguated considering physical constraints, *i.e.* the space line must lie in the visible part of the space.

The solution proposed in [16] and later resumed by [1, 10] employs the Plücker representation and requires to compute the Singular Value Decomposition of the 6x4 matrix of Plücker coordinates of the four corresponding rays.

In our comparison we instead adopted the euclidean approach described in [5] which requires to solve a second degree equation in one unknown.

### 3.1. Localization by minimizing rays distance

The previous method may suffer from noise since it use the minimum number of rays: the localized line might not cross all the other viewing rays mainly because of calibration error and noise which occurs in the image formation process.

In order to improve the robustness, the other viewing rays should also be used to validate the found solution. The previous result can be then used as an initial guess of a minimization process that refine the previous one in order to get an optimal line which is close to all the viewing rays. We devised an optimization method that minimize the sum of the square (euclidean) distances of the candidate space line from all the viewing rays. The distance between the candidate line and each ray is calculated as the minimum distance between two lines, *i.e.* the minimum distance between two points lying on the lines.

Generally a space line is described by six parameters. In order to reduce the dimensionality of the search space, we adopt a minimal parametrization derived from Roberts [13]: each line is described by four parameters  $x = [b_1, b_2, b_3, b_4]^T$  with the additional constraint that  $b_1^2 + b_2^2 \leq 1$ . In this parametrization  $b_1$  and  $b_2$  represent the  $x$  and  $y$  cosine directions of the line orientation while  $b_3$  and  $b_4$  are the  $xy$  coordinates of the intersection point with a convenient plane passing through the origin.

For this particular minimization method, in order to avoid the non-linearity of the constraints on  $b_1$  and  $b_2$  we adopt a slight different parametrization that employs the angle  $\alpha$  between  $b_1$  and  $b_2$ , and their norm  $\|b\| = \sqrt{b_1^2 + b_2^2}$ . Therefore classical linear minimization methods with linear constraint can be used for the optimization procedure.

### 3.2. Localization with RANSAC

A way to improve the robustness of the classical method is to exploit the RANSAC algorithm [7]. At each algorithm

iteration we randomly draw four rays to recover a candidate line. This line is then evaluated against all the other viewing rays by calculating the minimum distances. The candidate is accepted if the subset of viewing rays whose distance is below a given threshold is large enough.

The RANSAC approach is typically robust to noise and allows to find a line that better fit the given set of viewing rays.

#### 4. Localization using coplanar viewing rays

The first original method we propose exploits a pair of coplanar viewing rays. Given the plane associated to this pair, any two other rays of the viewing surface intersect it. These two intersection points univocally identify the space line. This method is attractive since it is very simple to implement and provide a univocal localization of the space line, as it does not require the disambiguation process between two solutions. On the other hand, it is not always applicable as it is not guaranteed that a pair of coplanar rays exists.

While determining the viewing ray associated to a contour point is straightforward from the system calibration, finding two coplanar viewing rays requires to match the rays associated to the contour points. Given a viewing ray  $r$  associated to a point  $p$  on the image contour  $c$  of the line, we devised the following procedure in order to find a corresponding coplanar viewing ray:

- a) for each point  $p_i \in c$  calculate the relevant (signed) minimum distance between the ray  $r_i$  (associated to  $p_i$ ) and  $r$ . If the distance is equal to zero, then the rays intersect in one point and are coplanar. Otherwise they are skew.
- b) The viewing rays associated to points of  $c$  close to  $p$  will possibly have a distance value near zero, but they are not coplanar. In order to choose more robustly a reliable coplanar viewing ray, we consider the trend of the distance value along the contour  $c$  and then we consider only the viewing rays whose distance is near the zero-crossing point of the trend.
- c) Interpolate the contour points associated to the found viewing rays with a cubic spline and then find the contour point  $p_x$  whose associated viewing ray  $r_x$  has minimum distance from  $r$ .
- d) The viewing ray  $r_x$  associated to  $p_x$  is retained the viewing ray coplanar to  $r$ .

Once a pair is found, we determine the 3D intersection points of all other viewing rays with the plane and then robustly fit the points to get the space line.

#### 5. Plücker localization

The second original method we propose is based on a constrained non linear minimization whose error function is

not based on euclidean distance. Indeed, if the space line is far from the camera mirror then large variations in its position and inclination could be reflected in very small changes in its projected image curve: a good error function should take into consideration this issue by reducing the weight of the error for distant configurations. Unfortunately this property does not hold for error functions based on euclidean distances, thus these methods will perform poorly in localizing distant space lines. Moreover, as we have stated, solutions represented by lines which intersect or are behind the mirror surface should be avoided since are not physically valid.

To tackle these problems we use a constrained non-linear minimization procedure which takes into consideration the bilinear operator between Plücker vectors<sup>1</sup>: given a current candidate solution  $x$ , expressed by a generic Plücker vector  $l_x$ , the bilinear operator  $side(l_x, l_i)$  will be zero if the two line intersects, where  $l_i$  is the normalized Plücker vector of the  $i$ -th viewing ray.

Thus we may use the following normalized squared sum as error function:

$$e(l_x) = \sum_i \frac{side(l_x, l_i)^2}{\|l_x\|^2}$$

The minimization is subject to a set of constraints which state that the candidate solution intersects each ray externally w.r.t. the mirror surface. This minimization contains local minima, but the candidate lines are bounded to the valid subspace of  $\mathbb{R}^3$  where the correct solution should lay.

We require a line parametrization which allows only valid line to be represented since the non-linear constraints we adopted might be evaluated only for real lines. Thus we cannot use directly the six Plücker vector parameters, which requires that  $side(l_x, l_x) = 0$ , or the original Roberts parametrization, which bounds the solution inside the hyper-cylinder  $b_1^2 + b_2^2 \leq 1$  in  $\mathbb{R}^4$

Moreover, in this latter case, the two endpoints of any diameter of the hyper-cylinder represent the same space line. This fact implies that the mapping between the Roberts parameters space and the set of space lines contains discontinuities (two lines almost parallel to the  $z = 0$  plane, which may be considered close to each other, are described by two vectors which are distant from each other but close to the validity border).

In order to tackle this problem we replace the first two Roberts coordinates with two angles describing the line orientation in radians. This new mapping, although non-linear, does represent a continuous function but introduces multiple local minima since the error function becomes periodic.

This line representation (and the original Roberts one) suffers from the dependence on the coordinate system con-

<sup>1</sup>The bilinear operator between two Plücker vector  $a$  and  $b$  is defined as  $side(a, b) = a_1b_6 + a_2b_5 + a_3b_4 + a_4b_3 + a_5b_2 + a_6b_1$

sidered. Small changes in the first two parameters (angles or cosines) may be reflected in large variations of the line position and orientation w.r.t. the viewing surface. To overcome the problem we perform a roto-translation  $T$  to the coordinate system which brings the origin to the intersection of one of the viewing rays with the mirror surface, the  $y$ -axis to the same ray orientation and the  $x$ -axis pointing away from the viewing surface. Notice that, with this new coordinate system, the solution should lie close to the  $x = 0$  plane. Once the optimization is completed the recovered solution has to be roto-translated back to the original coordinate system via  $T^{-1}$ .

## 6. Quality of the associated viewing surfaces

If the viewing surface of the considered line is a quadric surface the reconstruction is not possible since there are infinite valid solutions. A practical issue in catadioptric systems is that the viewing surfaces are close to quadric forms. In this case small errors in the image curve points extraction are reflected into a poor reconstruction even if the associated error of the robust method adopted tends to be small. Thus, there is the need to evaluate whether the viewing surface allows for a good reconstruction and in particular how close it is to a quadric surface.

Consider a set of viewing rays of a quadric surface  $S$  and a plane  $\pi$  in a generic position. In this case the envelope of the viewing rays projections on  $\pi$  is represented by a conic section.

By contrast we assume that, for a generic viewing surface, in most of the cases the envelope  $E$  of the viewing rays projections on a generic plane  $\pi$  will not be represented by a conic section. We may estimate how close  $E$  is to a quadric form in order to obtain an index of the surface validity. In particular, given the set of rays projections we can estimate the associated closest dual conic  $C^*$  by calculating the Sampson error  $e_s(C^*)$  [14]. This error may be evaluated on different planes in order to obtain a robust estimation of the quadric similarity of the viewing surface.

We draw from a uniform distribution  $n$  versors in  $\mathbb{R}^3$  representing the planes normals, project all rays to the corresponding planes passing through the origin, and evaluate the Sampson error. The mean value

$$\frac{1}{n} \cdot \sum_{i=1}^n e_s(C_i^*)$$

represents the reconstruction validity for viewing surface; the higher the value the better should be the reconstruction obtained, since a good reconstruction is given by a line which lie on a viewing surface which is far from being a quadric surface, and thus which possesses a high figure value.

## 7. Experimental results

First, the five methods have been implemented and validated with synthetic images rendered with Pov-Ray [12]. Then, their localization performances have been compared against a dataset of real images captured with a camera placed in a general position w.r.t. a conic mirror. As a target we chose a panel with a line pattern (see Figure 1) in order to have a reliable world reference and also to simplify the line image extraction process.

For these experiments we followed a two-step calibration, exploiting the method proposed by Mashita *et al.* [11] because of its simplicity. First, we estimated the intrinsic camera parameters using the Matlab Calibration Toolbox [3], then we estimated the mirror posture w.r.t. the camera, using the ellipse in the image corresponding to the boundary of the mirror. The accuracy of this localization technique relies on sufficient accuracy of the mirror shape and it may introduce some errors.

In order to evaluate the localization accuracy, we needed a ground truth for the space lines. Since it is not easily retrievable, we used the following procedure to recover a reliable ground truth. Given that the base of the target panel is placed on the same plane of the mirror base and it is directly visible from the perspective camera, we first localized the base of the panel and then the 3D plane  $\pi$  containing the panel. Finally we intersected the viewing surface associated to each line with  $\pi$ , thus getting the 3D equations of the space lines.

For each image we manually extracted the contour points of the lines and calculated the relevant sets of viewing rays exploiting calibration information. We then used these sets to localize the space lines with the five methods. For the classical method we used by default four equally angular spaced viewing rays. The solution provided is also used as starting guess for the minimization method. For the Plücker method we consider four random rays to get an initial solution and then we started the non linear minimization procedure. Since the methods exploiting coplanar viewing rays is not always applicable, we pick a random ray and look for a coplanar one. If it does not exist we repeated the procedure  $N = 100$  times before giving up.

Table 1 collects the localization results. For each line of each image in the dataset we reported the accuracy of the method in terms of angular error  $\epsilon_\alpha$  (in degree) and distance  $d_e$  from the ground truth (in cm). As distance measure we chose the mean value of the euclidean distance between the extrema of the reconstructed line and those of the space line. We also reported the Quadric Similarity QS index and the distance  $d_c$  (in cm) of the space line from the camera. Figure 2 reports the plot of the angular error for each line together with the QS index of the relevant viewing surface.

As stated in Section 4, the method employing coplanar rays is not always applicable. In our dataset it was applica-

ble only for lines in `img05` and `img03`. In this cases, however, the accuracy is quite good as the angular errors are always less than  $1^\circ$  and the mean distance errors are within 1 cm.

The results obtained with the classical method are (not surprisingly) controversial as sometimes the angular errors are rather good (even less than  $1^\circ$  in line 10 and 5 of `img10`) while in other cases they diverge up to  $20^\circ$  (line 18 of `img14`). The distance errors are usually larger than the previous methods, spreading from 1 up to 20 cm. This clearly shows the main drawback of this approach which is not robust to noise as outliers lead the solution to diverge. On the other hand, the minimization method that uses this solution as initial guess does not show better results, mainly because this approach is affected by local minima: even if the viewing surfaces are neither planar nor ruled quadrics, they are close to quadrics and so there are lots of minima that contain feasible lines.

The accuracy of the RANSAC method and the Plücker method are quite good as the maximum angular errors are about  $4^\circ$  for line 12 and 18 of `img14`, while for all other lines the errors are even much smaller.

As stated in Section 6, we observe that higher values of the QS index corresponds to a better confidence in localization, due to the fact that the viewing surface is far from being quadric. For instance, the highest QS index values obtained for the viewing surfaces of lines in `img03` lead to a more reliable localization results.

## 8. Conclusions

In this paper we proposed two novel localization algorithms for space lines from a single catadioptric image, one based on a pair of coplanar viewing rays while the other one is a non linear optimization procedure with a suitable Plücker representation of lines.

We compared the proposed methods with a classical localization method recently proposed in literature. This method has been proved to be less accurate mainly because of noise. Moreover, even if the solution provided is refined with a minimization method, the accuracy is rarely improved because the minimization procedure get into local minima.

The RANSAC technique performs much better and allows to keep the localization errors very small. The two original methods we propose have been proved to be very accurate and robust as well. The coplanar method is very attractive since it is very easy to implement but it can not be always applied because it is not guarantee that there is coplanar viewing rays in the same viewing surface. The Plücker method, on the other hand, is always applicable and guarantees a quite good accuracy.

## References

- [1] S. Avidan and A. Shashua. Trajectory triangulation: 3D reconstruction of moving points from a monocular image sequence. *IEEE Transactions on Pattern Analysis and Machine Intelligence*, 22(4):348–357, April 2000. 2
- [2] S. Baker and S. K. Nayar. A theory of single-viewpoint catadioptric image formation. *International Journal of Computer Vision*, 35(2):175–196, November 1999. 1
- [3] J. Y. Bouguet. Camera calibration toolbox for matlab. <http://www.vision.caltech.edu/bouguetj>. 4
- [4] H. Bronnimann, H. Everett, S. Lazard, F. Sottile, and S. Whitesides. Transversals to line segments in three-dimensional space. *Discrete Computational Geometry*, 34(3):381–390, 2005. 1
- [5] V. Caglioti and S. Gasparini. On the localization of straight lines in 3D space from single 2D images. In *Proceedings of the IEEE International Conference on Computer Vision and Pattern Recognition (CVPR '05)*, volume 1, pages 1129–1134, Los Alamitos, CA, USA, 20–25 June 2005. IEEE Computer Society. 2
- [6] V. Caglioti and S. Gasparini. “How many planar viewing surfaces are there in noncentral catadioptric cameras?” Towards single-image localization of space lines. In *Proceedings of the IEEE International Conference on Computer Vision and Pattern Recognition (CVPR '06)*, volume 1, pages 1266–1273, Los Alamitos, CA, USA, 17–22 June 2006. IEEE Computer Society. 1, 2
- [7] M. A. Fischler and R. C. Bolles. Random sample consensus: a paradigm for model fitting with applications to image analysis and automated cartography. *Communication of ACM*, 24(6):381–395, 1981. 2
- [8] T. Hassner and R. Basri. Example based 3d reconstruction from single 2d images. In *Proceedings of the 2006 Conference on Computer Vision and Pattern Recognition Workshop (CVPRW06)*, page 15. IEEE Computer Society, June 2006. 1
- [9] D. Hilbert and S. Cohn-Vossen. *Geometry and the Imagination*. Chelsea Publishing Co., New York: Chelsea, 1932. 1, 2
- [10] D. Lanman, M. Wachs, G. Taubin, and F. Cukierman. Reconstructing a 3d line from a single catadioptric image. In *Proceedings of the Third International Symposium on 3D Data Processing, Visualization, and Transmission*, pages 89–96, June 2006. 2
- [11] T. Mashita, Y. Iwai, and M. Yachida. Calibration method for misaligned catadioptric camera. In *Proceedings of the 6th Workshop on Omnidirectional Vision (OMNIVIS 2005)*, 2005. available online at <http://www.eecs.berkeley.edu/~cgeyer/OMNIVIS05/>. 4
- [12] POV Team. Persistency of vision ray tracer (POV-Ray). <http://www.povray.org>. 4
- [13] K. Roberts. A new representation for a line. In *Proceedings of the IEEE International Conference on Computer Vision and Pattern Recognition (CVPR '88)*, pages 635–640, Los Alamitos, CA, USA, 5–9 June 1988. IEEE Computer Society. 2
- [14] P. Sampson. Fitting conic sections to ‘very scattered’ data: An iterative refinement of the bookstein algorithm. *Computer Graphics Image Processing*, 18(1):97–108, January 1982. 4
- [15] P. Sturm. A method for 3D reconstruction of piecewise planar objects from single panoramic images. In *Proceedings of the 1st Workshop on Omnidirectional Vision (OMNIVIS 2000)*, pages 119–126, Los Alamitos, CA, USA, June 2000. IEEE Computer Society. 1
- [16] S. Teller and M. Hohmeyer. Determining the lines through four lines. *Journal of graphics tools*, 4(3):11–22, 1999. 1, 2
- [17] M. Wilczkowiak, E. Boyer, and P. Sturm. Camera calibration and 3d reconstruction from single images using parallelepipeds. In *Proceedings of the IEEE International Conference on Computer Vision (ICCV '01)*, volume 1, pages 142–148, 7–14 July 2001. 1



Figure 1. The dataset.

	$d_c$	QS	4Lines		Minimization		Ransac		Plücker		Coplanar	
			$\epsilon_\alpha$	$d_e$	$\epsilon_\alpha$	$d_e$	$\epsilon_\alpha$	$d_e$	$\epsilon_\alpha$	$d_e$	$\epsilon_\alpha$	$d_e$
img03_line5	113,7	2,24E-04	0,73	0,25	0,72	0,24	0,33	0,13	0,05	0,02	0,08	0,35
img03_line6	112,3	4,48E-04	3,61	1,20	3,60	1,20	0,12	0,45	0,26	0,68	0,29	0,82
img03_line7	112,3	3,67E-04	3,61	1,21	3,61	1,20	0,18	0,32	0,39	0,66	0,11	0,63
img05_line8	97,1	8,99E-06	1,01	2,22	0,91	2,58	0,27	0,45	0,37	2,08	0,94	0,90
img05_line9	95,6	1,00E-05	4,05	2,50	4,09	2,66	0,48	0,20	0,84	0,37	0,94	0,59
img05_line12	91,1	9,27E-06	0,72	3,53	0,81	3,74	0,67	0,22	0,66	0,20	0,60	0,67
img05_line10	94,8	9,08E-06	8,71	2,52	8,93	2,55	0,49	0,34	0,36	2,29	0,45	0,37
img10_line6	84,0	2,31E-05	5,08	2,74	4,78	2,58	1,98	1,17	1,33	0,83	n.a.	n.a.
img10_line8	83,2	2,37E-05	2,98	2,23	2,74	2,30	1,11	1,52	0,95	1,57	n.a.	n.a.
img10_line10	82,1	9,74E-05	0,26	1,50	0,20	0,12	0,64	0,15	0,33	0,37	n.a.	n.a.
img10_line12	81,0	1,64E-04	1,63	2,30	1,38	1,80	0,38	0,54	0,42	0,65	n.a.	n.a.
img14_line10	61,3	3,09E-05	9,18	10,29	9,08	10,35	1,19	1,08	2,23	0,52	n.a.	n.a.
img14_line12	59,9	3,57E-05	10,79	12,08	10,76	11,58	3,77	1,46	5,07	1,73	n.a.	n.a.
img14_line14	57,2	2,52E-05	9,80	18,47	10,72	20,35	1,91	1,52	1,88	1,37	n.a.	n.a.
img14_line16	55,3	2,98E-05	8,97	11,06	8,89	11,11	1,65	2,01	1,92	1,90	n.a.	n.a.
img14_line18	53,8	2,81E-05	21,56	18,89	21,35	18,87	4,17	6,58	3,09	2,50	n.a.	n.a.

Table 1. The accuracy of the proposed reconstruction methods. For each line of each image of the dataset we report the distance  $d_c$  (in cm) of the space line from the camera, the quadric similarity index QS, the angular error  $\epsilon_\alpha$  (in deg) and the mean distance between extrema  $d_e$  for each localization method.

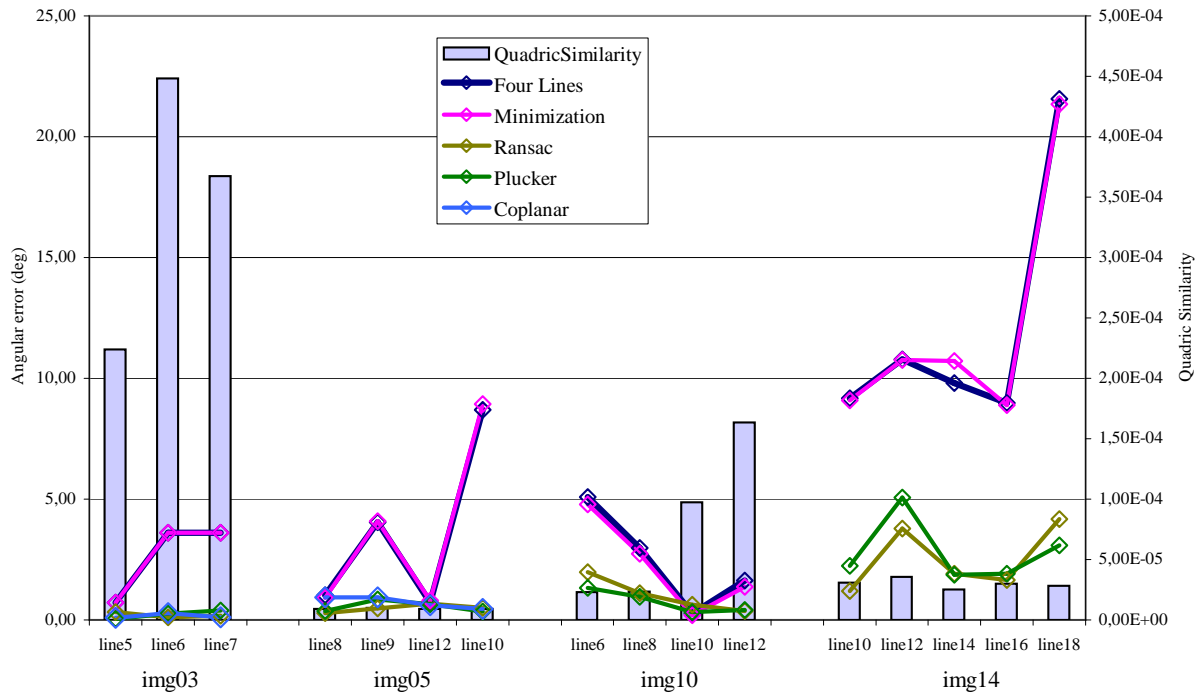


Figure 2. The graph plots the angular error  $\epsilon_\alpha$  for each reconstruction method on the images of the dataset. For each line also the quadric similarity index is plotted (light blue bars).